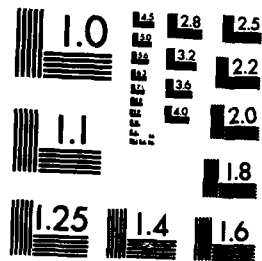


AD-A181 050 INTERACTIVE BUCKLING EFFECTS IN STIFFENED GRP PANELS 1/1
(U) ADMIRALTY RESEARCH ESTABLISHMENT DUNFERMLINE
(SCOTLAND) C S SMITH ET AL. MAR 87 ARE-TM-(UMS)-87204
UNCLASSIFIED DRIC-BR-102030 F/G 13/3 NL





MICROCOPY RESOLUTION TEST CHART
NATIONAL BUREAU OF STANDARDS-1963-A

AD-A181 050

UNLIMITED

ARE TM (UMS) 87204

INTERACTIVE BUCKLING EFFECTS IN STIFFENED
FRP PANELS (UL)

BY

C S SMITH AND R S DOW

Summary (UL)

Results are described of a numerical study of the initial compressive buckling and post-buckling behaviour of GRP panels reinforced by longitudinal hat-section stiffeners. Particular reference is made to the effects of interaction between local buckling of the panel laminate and overall, column-like buckling involving bending of the stiffeners. Conclusions are reached regarding the influence of interactive effects on collapse strength and recommendations are made on allowance for these effects in design. (Great Britain).

Accession For	
NTIS GRA&I	
DTIC TAB	
Unannounced <input type="checkbox"/>	
Justification	
By _____	
Distribution/	
Availability Codes	
Dist	Avail and/or Special
A-1	

ADMIRALTY RESEARCH ESTABLISHMENT
Procurement Executive, Ministry of Defence
Dunfermline, Fife

C
Copyright
Controller HMSO London
1987

- 1 -

UNLIMITED

UNLIMITED

CONTENTS

	<u>Page No</u>
TITLE	1
INTRODUCTION	3
METHODS OF ANALYSIS	4-6
SCOPE OF ANALYSIS	6-7
DISCUSSION OF RESULTS	7-10
Initial Buckling Behaviour	7
Nonlinear and Post-buckling Behaviour	8
Interactive Effects	8-10
DESIGN IMPLICATIONS	10
ACKNOWLEDGEMENT	10
REFERENCES 1-9	11
TABLE 1	12
FIGURES 1-10	



UNLIMITED

INTERACTIVE BUCKLING EFFECTS IN STIFFENED FRP PANELS

INTRODUCTION

1. Stiffened GRP panels, employing hat-section stiffeners aligned longitudinally in the direction of dominant load, have been adopted in the deck and bottom-shell structure of new minehunters currently under development for the Royal Navy (1)*. A theoretical and experimental investigation (2) has identified various forms of instability which may occur in panels of this type under longitudinal compression and has examined the relationship between initial buckling modes and post-buckling and collapse behaviour. It appeared that significant interactions could occur in some cases between local and overall buckling modes, influencing both initial buckling and post-buckling behaviour and hence possibly requiring special treatment in design. The purpose of the present report is to describe a further study in which such interactive effects were examined by numerical analysis of some panels in which the relationship between local and overall, column-like buckling was varied systematically by adjusting the panel geometry.

METHODS OF ANALYSIS

2. Methods of evaluating the initial buckling behaviour of stiffened FRP panels have been described previously (2) but will be summarized below for completeness.

3. A typical GRP deck or shell panel, reinforced by longitudinal stiffeners of trapezoidal, top-hat section, is shown in Figure 1. Strips of laminate forming the panel cross-section may be related to x and y-axes parallel to their longitudinal and transverse edges. For most marine-type GRP laminates based on chopped-strand, woven-roving or unidirectional reinforcement it is possible to assume that each strip of laminate is orthotropic with principal directions of elasticity parallel to its edges and that plies of reinforcement are stacked symmetrically about mid-thickness so that no direct coupling occurs between membrane and bending deformations. In-plane deformations of each strip then satisfy the orthotropic plane stress-strain relationship

$$\begin{bmatrix} \epsilon_x \\ \epsilon_y \\ \gamma_{xy} \end{bmatrix} = \begin{bmatrix} 1/E_x & -u_x/E_y & 0 \\ -u_y/E_x & 1/E_y & 0 \\ 0 & 0 & 1/G_{xy} \end{bmatrix} \begin{bmatrix} \sigma_x \\ \sigma_y \\ \tau_{xy} \end{bmatrix} \quad [1]$$

where E_x , E_y , G_{xy} , u_x and u_y are Young's moduli, shear modulus and Poisson ratios referring to the principal directions. The moment-curvature relationship for the strip is

*() References on Page 11

UNLIMITED

$$\begin{bmatrix} m_x \\ m_y \\ m_{xy} \end{bmatrix} = - \begin{bmatrix} D_x & \mu_x D_x & 0 \\ \mu_y D_y & D_y & 0 \\ 0 & 0 & D_{xy} \end{bmatrix} \begin{bmatrix} \frac{\partial^2 w}{\partial x^2} \\ \frac{\partial^2 w}{\partial y^2} \\ \frac{\partial^2 w}{\partial x \partial y} \end{bmatrix} \quad [2]$$

where

$$D_x = \frac{E_x h^3}{12(1-\mu_x \mu_y)} \quad \text{and} \quad D_y = \frac{E_y h^3}{12(1-\mu_x \mu_y)}$$

are flexural rigidities per unit width in x and y-directions.

$D_{xy} = G_{xy} h^3 / 12$ is the twisting rigidity and h is the laminate thickness.

4. In the presence of a uniform destabilising stress σ'_x as shown in Figure 1, the equation governing small bending displacements w of a laminate strip is

$$D_x \frac{\partial^4 w}{\partial x^4} + 2H \frac{\partial^4 w}{\partial x^2 \partial y^2} + D_y \frac{\partial^4 w}{\partial y^4} + N_x \frac{\partial^2 w}{\partial x^2} = 0 \quad [3]$$

where $H = 2D_{xy} + \mu_x D_x$ and $N_x = \sigma'_x h$. A conservative estimate of local buckling stress for a stiffened panel may be obtained by applying to each element of the cross-section the formula

$$N_{xcr} = \frac{2\pi^2}{b^2} (H + \sqrt{D_x D_y}) \quad [4]$$

which corresponds to a solution of equation 3 for a long orthotropic strip of width b with simply supported edges: local buckling will tend to occur predominantly in the most slender element with a number of half-waves over the length (a) of the panel given approximately by

$$n = \frac{a}{b} \left(\frac{D_y}{D_x} \right)^{1/4} \quad [5]$$

UNLIMITED

A corresponding upper-bound estimate of initial buckling stress is provided by the formula for a long orthotropic strip with clamped edges (3)

$$N_{xcr} = \frac{\pi^2}{b^2} (2.4H + 4.6\sqrt{D_x D_y}) \quad [6]$$

in which case the preferred number of buckling half-waves is approximately

$$n = 1.5 \frac{a}{b} \left(\frac{D_y}{D_x} \right)^{1/4} \quad [7]$$

5. Initial buckling may also take the form of column-like instability of longitudinal stiffeners and attached shell laminate between heavy transverse frames or bulkheads. Ignoring rotational restraint provided by the transverse members, this buckling stress may be estimated using the Euler formula

$$\sigma_{xcr} = \frac{\pi^2 EI}{Aa^2} / \left(1 + \frac{\pi^2 EI}{a^2 G A_s} \right) \quad [8]$$

in which EI is the flexural rigidity of a stiffener with assumed effective breadth of shell, A is the total cross section of the stiffener with attached strip of shell, a is the spacing of transverse frames or bulkheads and $G A_s$ is the shear rigidity in which A_s may be taken as the area of the stiffener webs.

6. More accurate (theoretically exact) evaluation of initial buckling stresses may be achieved using folded-plate analysis, in which out-of-plane displacements of each strip satisfy equation 3 while in-plane displacements u and v satisfy the simultaneous equations

$$\frac{E_x}{1 - \nu_x \nu_y} \left[\frac{\partial^2 u}{\partial x^2} + \nu_x \frac{\partial^2 v}{\partial x \partial y} \right] + G_{xy} \left[\frac{\partial^2 v}{\partial x \partial y} - \frac{\partial^2 u}{\partial y^2} \right] = 0 \quad [9]$$

$$\frac{E_y}{1 - \nu_x \nu_y} \left[\frac{\partial^2 v}{\partial y^2} + \nu_y \frac{\partial^2 u}{\partial x \partial y} \right] + G_{xy} \left[\frac{\partial^2 v}{\partial x \partial y} + \frac{\partial^2 u}{\partial x^2} \right] - \sigma_x \frac{\partial^2 v}{\partial x^2} = 0 \quad [10]$$

UNLIMITED

If conditions of simple support are assumed at the ends of each strip ($v = \partial u / \partial x = 0$ and $w = \partial^2 w / \partial x^2 = 0$ at $x = 0, a$), solutions of equations 3, 9 and 10 are periodic in x and may be obtained in a way which accounts rigorously for interactions between strips of laminate forming a stiffened panel. Details of this analysis method, together with generalized computer programs developed independently by several investigators, are contained in References 4 to 8.

7. Evaluation of nonlinear and post-buckling behaviour, including the effects of imperfections, may be carried out using finite element analysis. Results described in the present paper were obtained using the general purpose nonlinear FE Program ASAS-NL, developed by Atkins R&D in collaboration with ARE, Dunfermline (9). Eight-node isoparametric quadrilateral shell elements were employed with constant anisotropic material properties as defined in Figure 2: large displacements were represented using an updated Lagrangean (moving coordinate) procedure with application of a modified Newton-Raphson iterative equilibrium correction. The adequacy of FE models was tested by obtaining estimates of initial buckling stresses and modes by linear eigenvalue analysis for comparison with exact folded-plate results.

SCOPE OF ANALYSIS

8. As a basis for evaluating interactions between local buckling and overall column-like buckling, analysis has been carried out for a series of longitudinally stiffened panels having the same cross-sectional geometry and material properties as the experimental panel L2 described in Reference 2. By varying the span a between transverse frames a range of structures was obtained in which initial column buckling stresses varied from less than, to substantially more than, local laminate buckling stresses. Panel dimensions and material properties are indicated in Figure 2. In addition to the experimental length ($a = 3060$ mm) spans of 1000, 1500, 2000, 2350, 2670 and 3500 mm were considered.

9. Initial buckling stresses were estimated approximately using equations 4 to 8, with the breadth b taken equal to the unsupported span between stiffener webs, and were computed accurately using folded-plate and finite element analysis. Stiffener flanges, which have been shown to influence local buckling significantly (2), were included in folded-plate and finite element models. Finite element analysis was also used to examine the nonlinear, post-buckling behaviour of panels including the influence of assumed imperfections. As shown in Figure 3, the finite element model referred to a single longitudinal stiffener with attached shell laminate extending over two half-spans $a/2$. Conditions of simple support were assumed at the position of the transverse frame EF, with a transverse plane of symmetry at mid-span position CD and a "moving" plane of symmetry at mid-span position AB: in this way account was taken of "continuous beam" interactions between adjoining spans. Longitudinal planes of symmetry AC and BD were assumed to occur mid-way between longitudinal stiffeners.

UNLIMITED

10. For the purpose of nonlinear analysis, initial deformation of each panel was assumed to have the form of the preferred local buckling mode with amplitude w_{op} , combined with an overall distortion of amplitude w_{os} having the form of the interframe column buckling mode. In each case two levels of imperfection were considered:

- (i) $w_{op}/a = 0.0005$, $w_{os}/a = 0.0013$ (corresponding approximately to maximum distortions measured in experimental Panel L2);
- (ii) $w_{op}/a = 0.00005$, $w_{os}/a = 0.00013$.

Initial deformation was taken to be antisymmetric about EF, positive (towards the stiffener) at AB and negative at CD. Analysis was carried out by incremental application of uniform end-shortening displacement on the plane AB of each panel.

DISCUSSION OF RESULTS

Initial Buckling Behaviour

11. Initial buckling stresses obtained from the approximate formulae and by folded-plate and FE analysis are listed in Table 1. A selection of corresponding buckling modes, obtained from the folded-plate solutions, is shown in Figure 4. Initial buckling stresses determined by FE eigenvalue analysis are generally within 5% of exact folded-plate values, lending some credibility to the FE model used in the nonlinear analysis.

12. As observed previously, critical stresses corresponding to local buckling of the shell laminate between stiffeners occur in closely spaced pairs; asymmetric modes (Type B) are usually (but not always) preceded by symmetric (Type A) modes. The latter generally involve virtually (but not exactly) zero displacement of stiffeners out of the panel plane. Type B modes involve distortion of stiffener cross-sections including some sideways bending of the stiffener tables. As might be expected, local buckling stresses and associated modal wavelengths are insensitive to the span a .

13. In the longest panel examined ($a = 3500$ mm) overall buckling occurs with virtually no local deformation at a critical stress 6% less than that given by the Euler formula (Equation. 8). As panel length is reduced the "column" mode becomes increasingly influenced by local deformation of the shell laminate and the associated critical stress falls progressively below the Euler value. In the shortest panel examined ($a = 1000$ mm) local shell deformation dominates the symmetric $n = 1$ mode and the critical stress is only 42% of the Euler value (lower than the column buckling stress for $a = 1500$ mm). In the case of a panel of length 2670 mm, chosen to give approximate equality of local ($n = 7$) and column ($n = 1$) buckling stresses, the column mode is only slightly influenced by local deformation.

UNLIMITED

Nonlinear and Post-buckling Behaviour

14. Nonlinear load-deformation relationships have been computed for four panels with lengths $a = 3500, 2670, 2000$ and 1000 mm, supplementing results reported previously (2) for the experimental panel L2 ($a = 3060$ mm), which were found to correlate fairly well with test data. Computed load-shortening curves, ie average compressive stresses σ_x' plotted against average strains ϵ_x' , are shown in Figure 5. Mid-span lateral displacements of stiffeners are shown in Figure 6: positive displacements (at section AB) are towards and negative displacements (at CD) away from the stiffener outstand.

15. For panels of length 3500, 2670 and 2000 mm, compressive loads reach their effective maxima at or just below initial overall buckling stress levels: collapse might be expected to occur at these load levels as a result of outer-fibre material failure at a strain of about 0.02. Computed outer-fibre stiffener strains ϵ_x' at mid-span positions (AB and CD) are shown for each panel in Figure 7. Computed deformation of the longest panel at peak load is shown in Figure 8.

16. In the shortest panel ($a = 1000$ mm), σ_x' reaches a plateau at about 120 MPa, substantially higher than the initial $n = 1$ buckling stresses but lower than the equation 8 Euler stress (161 MPa): it appears that this load corresponds to "column" buckling in which overall flexural rigidity of the stiffened panel is reduced by loss of effective width caused by local buckling. Computed post-buckling deformations of the panel at average compressive stresses of 73 and 120 MPa are shown in Figure 9. It is evident from this diagram and from Figure 6 that significant "column" displacements develop at the higher load level. Short-wavelength compressive buckling of the stiffener webs is also apparent.

17. It may be noted from Figure 5 that in the two shortest panels ($a = 2000, 1000$ mm) occurrence of local buckling at an average stress of about 35 MPa results in a reduction of about 40% in the compressive stiffness ($d\sigma_x'/d\epsilon_x'$) of each panel. A further reduction of about 10% in axial stiffness occurs at an average stress of about 65 MPa, corresponding approximately to the symmetric $n = 1$ buckling stress. Associated distributions of compressive stress over the cross-section and loss of effective width are indicated in Figure 10. If the flexural rigidity EI of the cross-section is modified to reflect this loss of effective width, equation 8 gives an Euler buckling stress of 132 MPa, about 10% higher than the load plateau indicated by nonlinear analysis.

Interactive Effects

18. Interactive buckling effects in a longitudinally stiffened FRP panel under longitudinal compression may be summarized as follows.

UNLIMITED

- (i) Buckling and post-buckling behaviour will usually be strongly influenced by coupling between strips of laminate forming the shell and stiffeners: this effect invalidates the use of simple formulae for evaluation of local buckling stresses (except to provide crude upper and lower bounds) and can only be accounted for by use of folded-plate, finite-element or finite-strip analysis. In long panels for which the overall ($n = 1$) initial buckling stress is of the same order as or less than the local buckling stress and in which the preferred local buckling wavelength is a small fraction of the span a , interaction between overall and local initial buckling is slight and the former may be examined with reasonable accuracy using the Euler formula. In short panels, where the local initial buckling stress is substantially less than the overall buckling stress and the preferred number of buckling half-waves (n) is small, overall instability may be strongly influenced by local deformation and may occur at a stress substantially less than the Euler value.
- (ii) Local buckling of the shell laminate between stiffeners is associated with loss of effective width, as illustrated in Figure 10, causing an increase in stiffener stress which will tend to accelerate outer-fibre material failure, together with a reduction in the incremental (tangent) flexural rigidity of the cross section affecting overall beam-column behaviour. This interactive effect is likely to be most marked in short stiffened panels where local buckling precedes overall instability. It is part of the reason why computed load-displacement curves (Figures 5 and 6) for panels with $a = 2000$ mm and $a = 2670$ mm reach a plateau, where collapse is likely to occur as a result of outer-fibre material failure, somewhat below the initial overall buckling stress. In the case of the shortest panel examined ($a = 1000$ mm) the overall ($n = 1$) buckling mode is dominated by local deformation; despite loss of effective width associated with local buckling, computed load-displacement curves climb to a level well above the initial $n = 1$ buckling stress. It should be noted however (as demonstrated in Reference 2) that compressive failure of a short panel may be caused prematurely by debonding of stiffeners induced by local buckling. Failure may also be precipitated by outer-fibre material failure of the locally buckled shell laminate.
- (iii) Bending of stiffeners associated with overall beam-column deformation may induce significant secondary compressive or tensile stress in the shell laminate between stiffeners. Where bending is towards the stiffener outstand such secondary stress is compressive, accelerating the occurrence of local buckling, loss of effective width and hence loss of overall flexural rigidity; where bending of stiffeners occurs

UNLIMITED

away from the outstand, secondary stress in the shell is tensile, tending to inhibit local buckling and loss of effective width. This effect is illustrated in Figure 8. A consequence is that lateral deformation of a multi-span stiffened panel tends to grow in an unsymmetrical manner with displacements towards the stiffener outstand exceeding displacements in the opposite direction. A two-span "continuous beam" model, as shown in Figure 3, is necessary to account for this form of behaviour in a numerical analysis. The effect is however found to be small for cases examined in the present paper: over the range of deformation shown in Figure 6 the maximum difference between "upward" and "downward" displacements is 10%.

- (iv) Approximate equality of critical stresses referring to local ($n = 7$) and column ($n = 1$) buckling modes (for the panel of length 2670 mm) does not appear to cause any special enhancement of the interaction effects discussed above.

DESIGN IMPLICATIONS

19. Current design recommendations for GRP ships (2) specify that factors of safety of 2.0 should be maintained against local and overall buckling of longitudinally stiffened panels under compressive load, reduced to 1.5 in the case of local buckling where positive measures, eg use of bolts or resilient adhesive with high peel strength, are employed to enhance stiffener attachment. As discussed in Reference 2, these factors are intended to account for typical initial imperfections but not for creep or for variability and long-term degradation of material properties, which should be allowed for separately by application of supplementary partial safety factors.

20. Various forms of interaction between local and overall buckling have been identified in the present numerical study. For panels with cross-sectional geometry similar to that of Figure 2 it appears that interaction effects are accounted for adequately by the margins indicated above and that no additional partial safety factor is necessary, even for the case where critical stresses referring to local and overall buckling modes are approximately equal. It seems likely that these conclusions will apply equally to most practical stiffened panels: scope clearly exists, however, for further exploration of interactive buckling effects in panels of differing geometry and for different patterns of initial deformation.

ACKNOWLEDGEMENT

21. Thanks are due to the authors' colleague, Mr W C Kirkwood, for assistance in carrying out computation.

UNLIMITED

REFERENCES

1. CHALMERS, D.W., OSBORN, R.J. and BUNNY, A., Hull construction of MCMVs in the United Kingdom, Inter. Symposium on Mine Warfare Vessels and Systems, RINA, London, June 1984.
2. SMITH, C.S. and DOW, R.S., Compressive strength of longitudinally stiffened GRP panels, Proc. 3rd Internat. Conf. on Composite Structures, Paisley, September 1985.
3. WITTRICK, W.H., Correlation between some stability problems for orthotropic and isotropic plates under biaxial and uniaxial direct stress, Aeronaut. Quarterly, 4, No. 1 (1952), 83.
4. SMITH, C.S., Elastic analysis of stiffened plating under lateral loading, Trans. RINA, 108 (1966).
5. SMITH, C.S., Bending, buckling and vibration of orthotropic plate-beam structures, J. Ship Res., 12, No. 4 (1968), 249-268.
6. WITTRICK, W.H., A unified approach to the initial buckling of stiffened panels in compression, Aeronaut. Quarterly, 19 (1968), 265-283.
7. WITTRICK, W.H. and WILLIAMS, F.W., Buckling and vibration of anisotropic or isotropic plate assemblies under combined loadings, Int. J. Mech. Sci., 16 (1974), 209-239.
8. VISWANATHAN, A.V., TAMEKUNI, M. and TRIPP, L.L., Elastic stability of biaxially loaded longitudinally stiffened composite structures, AIAA, ASME, SAE 14th Structures, Structural Dynamics and Materials Conference, Williamsburg Va, 1973.
9. ATKINS R&D, ASAS-NL User Manual, Version 12, December 1984.

UNLIMITED

TABLE 1 INITIAL BUCKLING MODES AND STRESSES (MPa)

Span a (mm)	Mode		Computed Results		Approximate Formulae		
	n	Type	Folded Plate	Finite Element	eqn. 4	eqn. 6	eqn. 8
3500	1	Euler	21.5	22.2	26.6(n=7)	50.1(n=10)	22.9
	8	A	35.0	34.3			
	8	B	35.4	35.2			
	9	A	34.9	35.8			
	9	B	35.5	36.0			
	10	A	35.9				
	10	B	37.0				
3060	1	Euler	27.4	28.2	26.6(n=6)	50.1(n=9)	29.4
	6	A	36.1	34.1			
	6	B	37.0	36.2			
	7	A	35.0	33.9			
	7	B	35.4	34.7			
	8	A	35.0	35.3			
	8	B	35.9	35.4			
	8						
2670	1	Euler	34.6	35.5	26.6(n=5)	50.1(n=8)	37.6
	6	A	35.1	35.0			
	6	B	35.4	34.5			
	7	A	35.0	35.5			
	7	B	36.0	35.7			
	8	A	36.7	38.0			
	8	B	37.8				
	8						
2350	1	Euler	42.6	43.5	26.6(n=4)	50.1(n=7)	47.0
	5	B	35.6	34.5			
	5	A	35.7	35.5			
	6	A	34.9	35.1			
	6	B	35.8	35.4			
	7	A	36.6	37.4			
	7	B	37.7	38.1			
2000	1	Euler	53.7		26.6(n=4)	50.1(n=6)	61.8
	4	B	35.9	35.3			
	4	A	36.7	36.6			
	5	A	34.8	34.9			
	5	B	35.7	35.2			
	6	A	36.7	37.7			
	6	B	37.9	38.0			
1500	1	Euler	71.5		26.6(n=3)	50.1(n=4)	96.5
	3	B	35.9				
	3	A	36.7				
	4	A	35.1				
	4	B	36.1				
	5	A	39.3				
	5	B	40.5				
1000	1	B	54.2	49.6	26.6(n=2)	50.1(n=2)	161.4
	1	A/Euler	67.8	67.5			
	2	B	35.9	36.4			
	2	A	36.7	36.8			
	3	A	36.7	36.9			
	3	B	37.9	37.7			
	3						

UNLIMITED

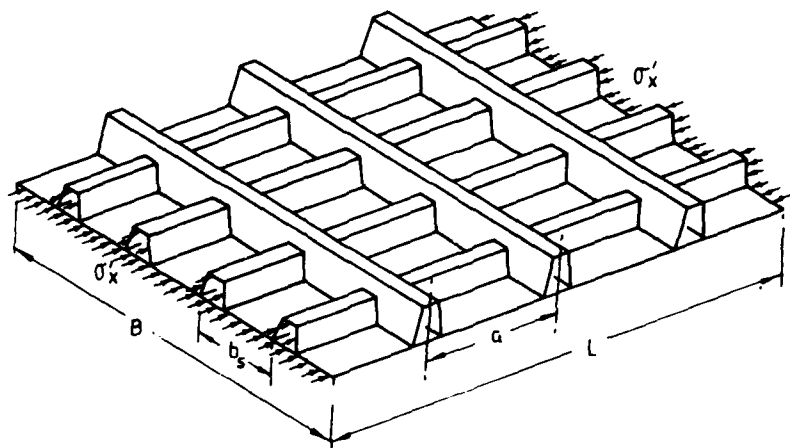
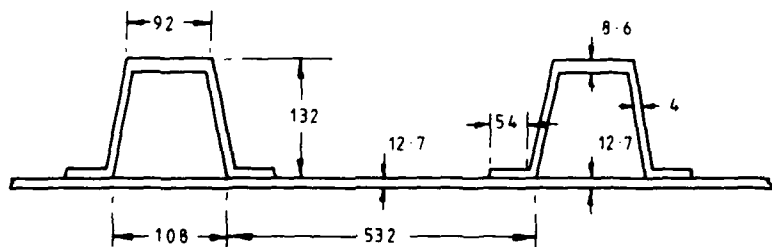


FIG 1 Longitudinally Compressed GRP Panel

DIMENSIONS IN mm



MEAN MATERIAL PROPERTIES	SHELL LAMINATE	STIFFENER TABLES	STIFFENER WEBS & FLANGES
E_x (GPa)	15.0	19.5	15.0
E_y (GPa)	13.5	11.9	13.5
G_{xy} (GPa)	3.45	3.45	3.45
μ_x	0.135	0.11	0.135
μ_y	0.15	0.18	0.15
FLEXURAL STRENGTH (MPa)	273	415	—

FIG 2 Panel Geometry and Material Properties

UNLIMITED

ARE TM (UMS) 87204

UNLIMITED

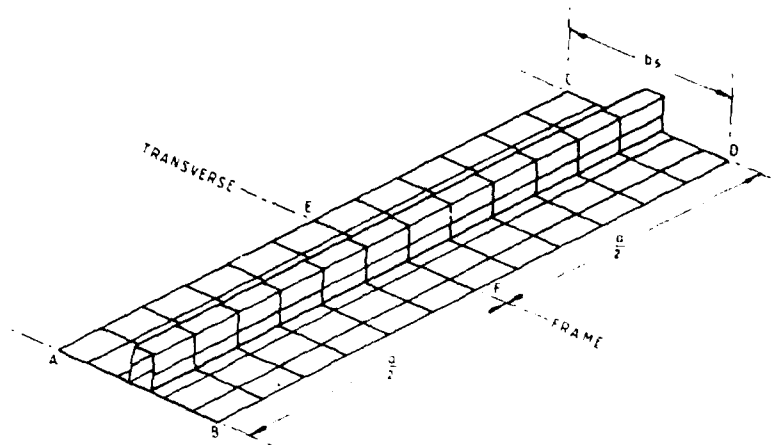


FIG 3 Finite Element Model of Stiffened Panel

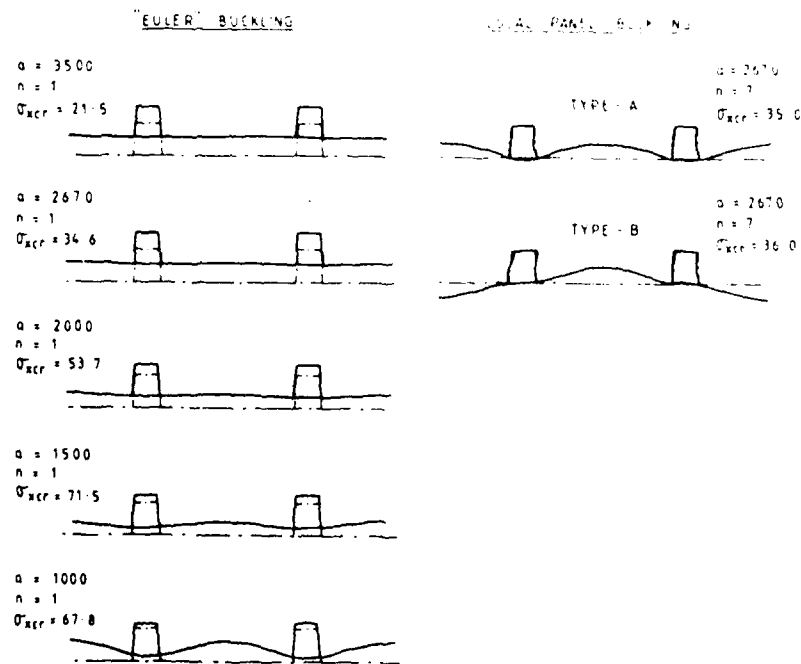


FIG 4 Selected Initial Buckling Modes Computed by Folded Plate Analysis

UNLIMITED

ARE TM (UMS) 87204

UNLIMITED

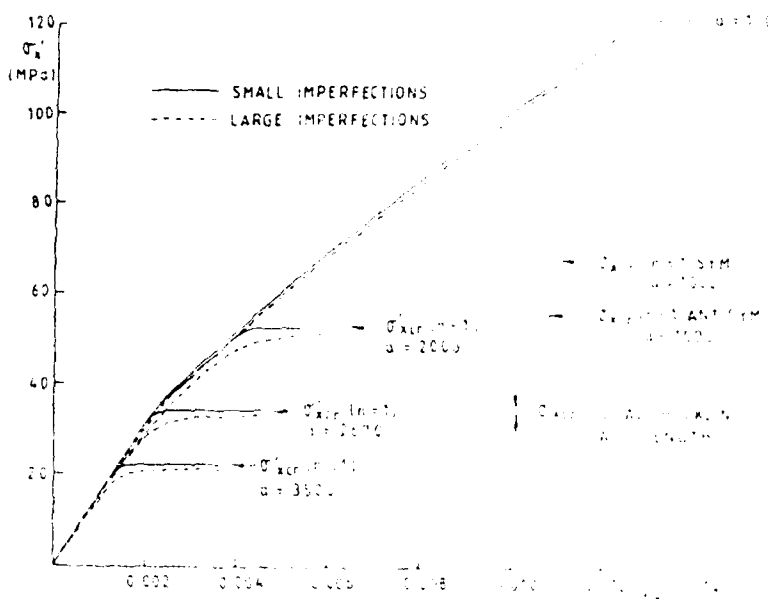


FIG 5 Load-Shortening Curves for Stiffened Panels



FIG 6 Mid-Span Lateral Displacement of Stiffeners

UNLIMITED

ARE TM (UMS) 87204

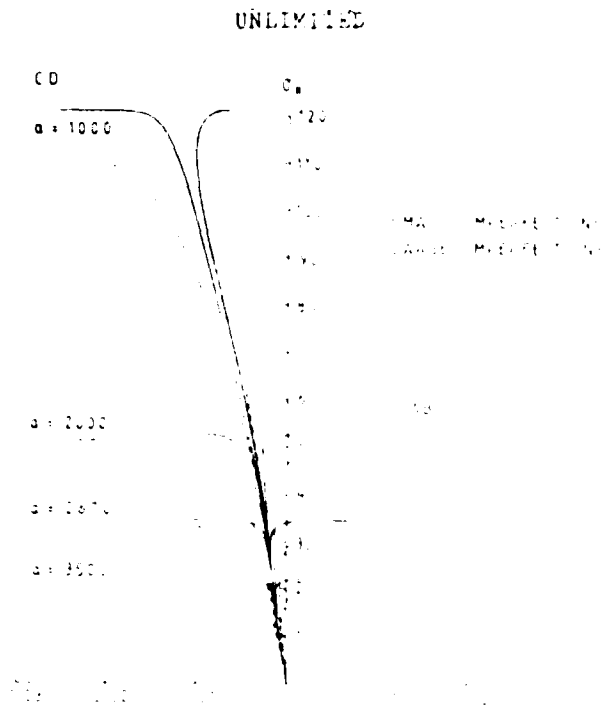


FIG. 7 Mid-Span Lateral-Flexure Stiffener Defl.

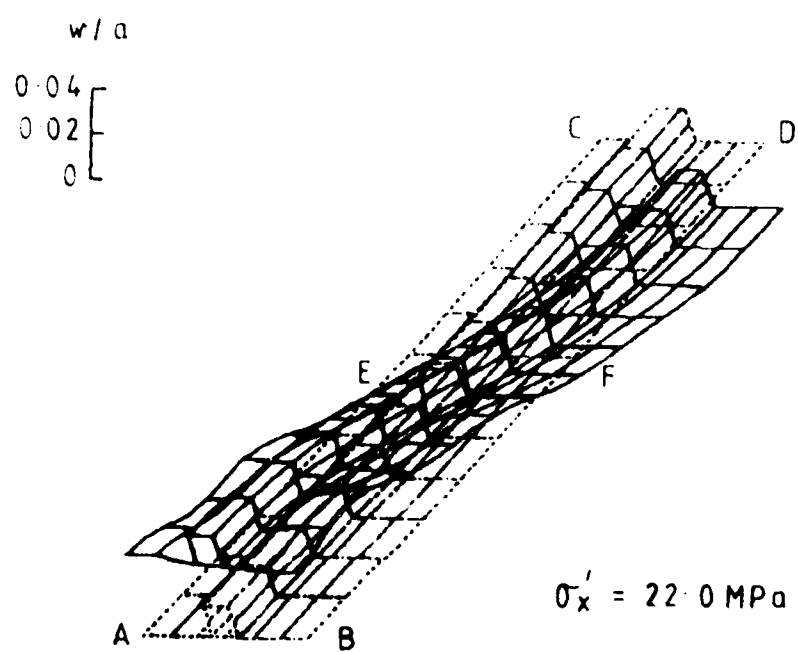


FIG. 8 Long Panel ($a = 3500$ mm): Computed Deformation Showing Local Buckling Caused by Secondary Compression

UNLIMITED

ARE TM (UMS) 87204

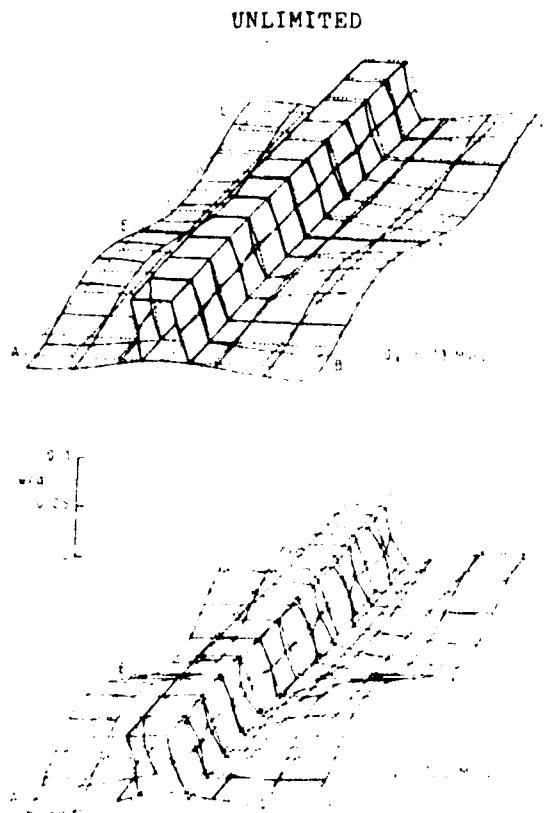


FIG 9 Short Panel ($a = 100 \text{ mm}$): Computed Post-buckling Deformations

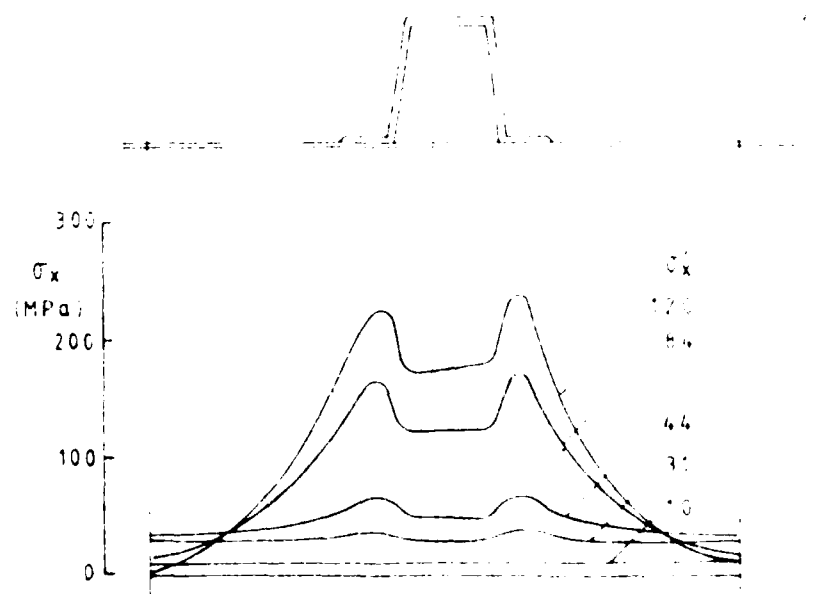


FIG 10 Compressive Stress Distributions Across Shell Laminate Showing Reduced Effective Width

UNLIMITED

ARE TM (UMS) 87204

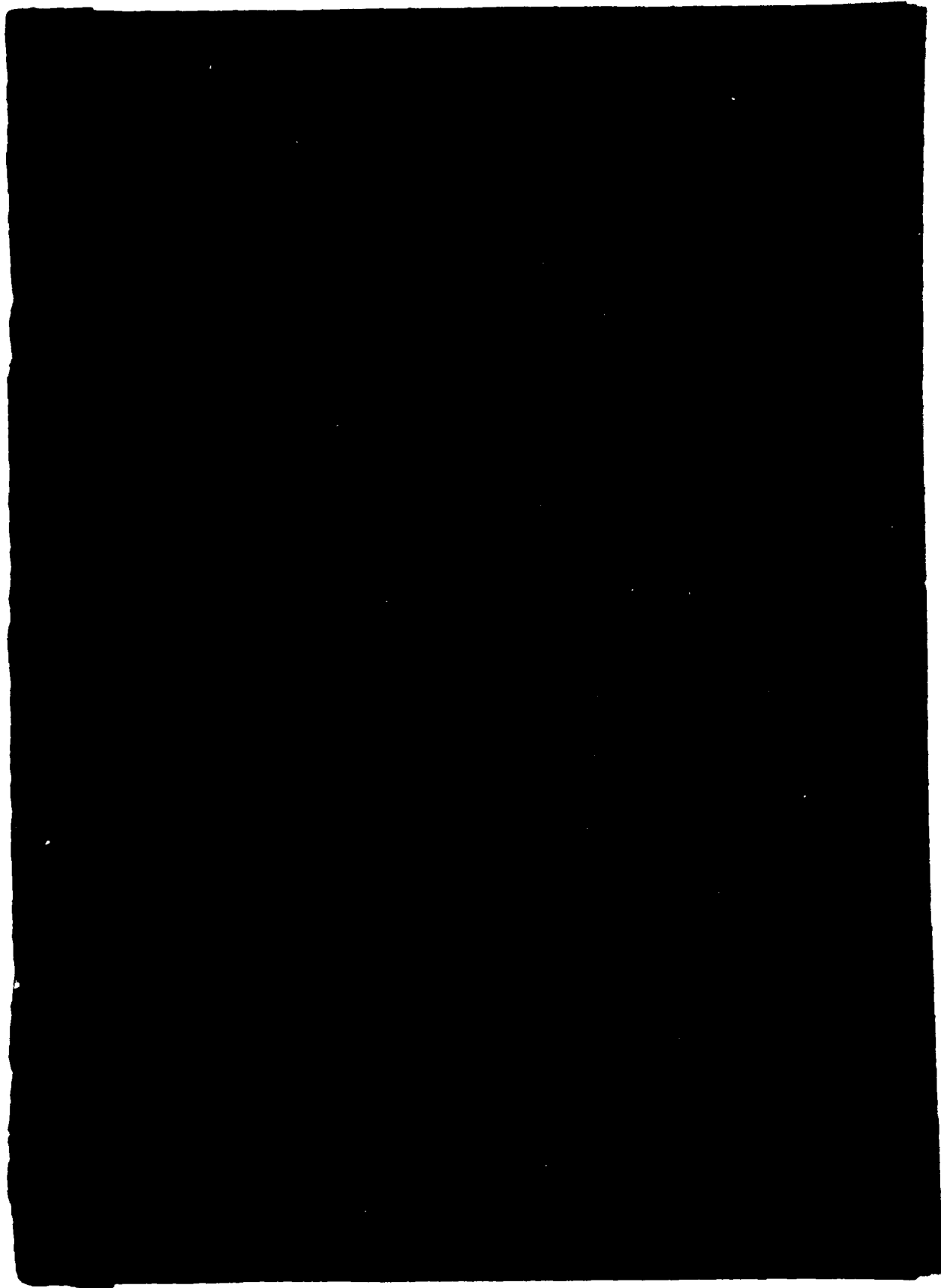
UNLIMITED

DISTRIBUTION

Copy No

1	DD(U), Portland
2	UM
3	CS(R)2e(Navy), Hayes, Middlesex
4	SCNO, Washington
5,6	CNA, Foxhill, Bath (Mr D Chalmers, NA123)
7,8	US Project Officer, IEP ABC 36
9-11	Canadian Project Officer, IEP ABC 36
12-34	DRIC, Glasgow
35	Sea Systems Library, Foxhill, Bath
36,37	Internal Copies (Dr Smith, Mr Dow)
38-45	ARC spares

UNLIMITED



END

DATE
FILMED

7-8-